Chin. J. Astron. Astrophys. Vol. 8 (2008), No. 3, 314–328
(*http://www.chjaa.org*)

Chinese Journal of
Astronomy and
Astrophysics

Detecting Very-High-Frequency Relic Gravitational Waves by a Waveguide *

Ming-Lei Tong and Yang Zhang

Centre for Astrophysics, University of Science and Technology of China, Hefei 230026, China
yzh@ustc.edu.cn

Received 2007 August 21; accepted 2007 November 26

Abstract The polarization vector (PV) of an electromagnetic wave (EW) will experience a rotation in a region of spacetime perturbed by gravitational waves (GWs). Based on this consideration, Cruise's group has built an annular waveguide to detect GWs. We give detailed calculations of the rotations of polarization vector of an EW caused by incident GWs from various directions and in various polarization states, and then analyze the accumulative effects on the polarization vector when the EW passes n cycles along the annular waveguide. We re-examine the feasibility and limitation of this method to detect GWs of high frequency around $100\,$MHz, in particular the relic gravitational waves (RGWs). By comparing the spectrum of RGWs in the accelerating universe with the detector sensitivity of the current waveguide, it is found that the amplitude of the RGWs is too low to be detected by the waveguide detectors currently operating. Possible ways of improvements on detection are suggested.

Key words: early universe — instrumentation: detectors — gravitational waves — polarization

1 INTRODUCTION

Gravitational wave (GW) is one of important predictions of general relativity. Although there has been some indirect evidence of GW radiation from the binary pulsar B1913+16 (Hulse & Taylor 1975; Weisberg & Taylor 2004), so far direct detection of GWs has not been accomplished. The GWs can have different frequencies generated by various kinds of sources. Currently, besides the conventional method of cryogenic resonant bar (Allen et al. 2000; Aston et al. 2001) a number of detectors using new techniques have been operating or under construction aiming at direct signals of GWs. For the frequency range $1 \sim 10^4$ Hz, the method of ground-based laser interferometers is applied, for example, in LIGO (Abramovici et al. 1992), Virgo (Bradaschia et al. 1990), and TAMA (Takahashi & Tagoshi 2004). For a lower frequency range, $10^{-4} \sim 1$ Hz, space-based laser interferometers can be used, such as the LISA (Jafry et al. 1994) that is being planned. For much lower frequencies $\sim 10^{-18}$ Hz, detections of CMB polarization of "magnetic" type might give direct evidence of the existence of GWs (Seljak & Zaldarriaga 1997; Kaminkowski et al. 1997; Pritchard & Kaminkowski 2005; Zhao & Zhang 2006; Baskaran et al. 2006). There have also been attempts to detect GWs of very high frequencies from MHz to GHz, employing various techniques, for instance, laser beam (Li et al. 2000, 2003, 2006). One interesting method proposed by Cruise uses an linearly polarized electromagnetic wave (EW) in a waveguide (Cruise 2000; Cruise & Ingley 2005, 2006). When a GW passes through the region of the waveguide, the polarization vector (PV) of the EW will generally undergo a rotation (Cruise 1983). A prototype GW detector has been built by Cruise & Ingley (2005, 2006), which mainly consists of one or several torus-shaped annular waveguides. This method has

* Supported by the National Natural Science Foundation of China.

the advantage of being capable, depending on the size of the waveguide, of detecting GWs in the very high frequency range of $10^6 \sim 10^9$ Hz, that was not covered by the laser interferometer method. Note that GWs in the frequency range $10^6 \sim 10^9$ Hz are generally not generated by usual astrophysical processes, such as binary neutron stars, binary black holes, merging of neutron stars or black holes, or collapse of stars (Grishchuk et al. 2001; Zhang et al. 2004).

However, the background of relic gravitational waves (RGWs) has a spectrum stretching over a whole range of $10^{-18} \sim 10^{11}$ Hz (Grishchuk 1975, 1997; Zhang et al. 2005). Depending on the frequency range, its different portions can be detected by different methods, e.g., the very low frequency range $10^{-18} \sim 10^{-16}$ Hz by the curl type of polarization in the CMB (Seljak & Zaldarriaga 1997; Kaminkowski et al. 1997; Pritchard & Kaminkowski 2005; Zhao & Zhang 2006; Baskaran et al. 2006), the low frequency range $10^{-3} \sim 10^{-2}$ Hz by LISA, the intermediate frequency range $10^2 \sim 10^3$ Hz is covered by LIGO, and the very high frequency range $10^6 \sim 10^9$ Hz can be the target of Cruise's EW polarization method. Therefore, one of the main objects of detection by the annular waveguide is the very high frequency RGWs. The detection of high frequency RGWs from MHz to GHz is complementary to the usual detectors working in the range of $10^{-4} \sim 10^4$ Hz. RGWs are stochastic background generated by the inflationary expansion of the early universe (Grishchuk 1975; Zhang et al. 2005a,b, 2006; Giovamini 1999; Zhao & Zhang 2006; Miao & Zhang 2007), and its spectrum depends sensitively on the inflationary and the subsequent reheating stages. Besides, the current accelerating expansion also affects both the shape and the amplitude of the RGW spectrum (Grishchuk 1975; Zhang et al. 2005a,b, 2006; Miao & Zhang 2007). The RGWs carry valuable information on the universe, therefore, their detection is much desired and might open a new window for astronomy.

In this paper we give an investigation of the rotation of the PV of EWs in a conducting torus caused by incident GWs, and explore the feasibility and limitation of Cruise's method of detecting GWs. First, we review the RGWs in the currently accelerating universe. Secondly, we present detailed calculations of the rotation of the PV of EWs in the waveguide caused by incoming GWs from various directions and in various polarization states, then we analyze the multi-cycle accumulating effect and the resonance when the circling frequency of EWs is nearly equal to that of the GWs'. Thirdly, we examine the possible detection of RGWs by the annular waveguide system around 100 MHz, and relate the predicted spectrum of the RGWs in the accelerating universe in regard to the sensitivity of the detector (Cruise & Ingley 2005, 2006). Finally, we state our conclusions and outline possible ways of improving the detection.

2 RELIC GRAVITATIONAL WAVES

In an expanding universe, RGWs can be regarded as a small perturbation of the Robertson-Walker metric,

$$\mathrm{d}s^2 = a^2(\tau)[-\mathrm{d}\tau^2 + (\delta_{ij} + h_{ij})\,\mathrm{d}x^i\mathrm{d}x^j], \tag{1}$$

where $a(\tau)$ is the scale factor, τ is the conformal time, and h_{ij} is a transverse-traceless representation of the RGWs,

$$\partial_i\, h^{ij} = 0, \qquad \delta^{ij}\, h_{ij} = 0\,. \tag{2}$$

Of the six components h_{ij} only two are independent (two polarization states). Generally, $|h_{ij}| \ll 1$. The wave equation for the RGWs is

$$\partial_\mu\,(\sqrt{-g}\,\partial^\mu\, h_{ij}(\mathbf{x},\tau)) = 0. \tag{3}$$

The solution of Equation (3), h_{ij}, and the spectrum $h(\nu, \tau_H)$ defined by

$$\langle h^{ij} h_{ij}\rangle = \int_0^\infty h^2(k,\tau_H)\frac{\mathrm{d}k}{k} \tag{4}$$

have been given for an accelerating universe (Zhang et al. 2005a,b, 2006; Miao & Zhang 2007; Grishchuk 2001). Figure 1 plots $h(\nu, \tau_H)$, defined by the acceleration parameter γ, the inflation parameter β, the reheating parameter β_s and the tensor/scalar ratio r. The redshift z_E at the time of equal dark energy and matter, τ_E, is given by

$$1 + z_E = \frac{a(\tau_H)}{a(\tau_E)} \simeq (\frac{\Omega_\Lambda}{\Omega_m})^{\frac{1}{3}}. \tag{5}$$

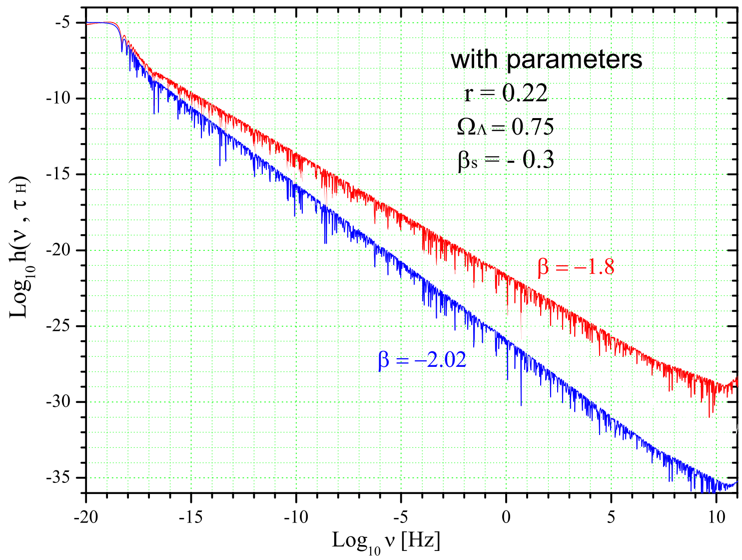

Fig. 1 Spectrum $h(\nu, \eta_H)$ of RGW in the accelerating universe (Miao & Zhang 2007; Zhang et al. 2006).

For detecting RGWs of frequencies $\sim 10^8$ Hz, we quote the analytic approximate spectrum in this range (Zhang et al. 2006):

$$h(k, \tau_H) \approx A_0 \Big(\frac{k_s}{k_H}\Big)^{\beta_s} \frac{k_H}{k_2} \Big(\frac{k}{k_H}\Big)^{\beta-\beta_s+1} \frac{1}{(1+z_E)^{3+\epsilon}}, \tag{6}$$

where k is the comoving wavenumber related to the physical frequency by $\nu = \frac{k}{2\pi a(\tau_H)}$, A_0 a constant determined by the CMB anisotropies (Seljak & Zaldarriaga 1997; Zhang et al. 2005a,b, 2006; Grishchuk 2001; Spergel et al. 2003), $\epsilon \equiv (1+\beta)(1-\gamma)/\gamma$ is a very small value, $k_H = 2\pi\gamma$ and $k_s \simeq 10^{26} k_H$. Note that the RGWs h_{ij} described above exist everywhere and for all the time in the universe. We may deem that the universe is filled with a stochastic background, consisting of all the modes of different wave-vectors, k^μ=(k^0, k^1, k^2, k^3). So the RGWs serve as an object for GW detection.

In the frequency range ~ 100 MHz for the waveguide detector, RGWs can be approximated as plane waves. A beam of monochromatic plane GWs with a wave-vector can be written in the following form (Misner et al. 1973)

$$h_{ij} = Re\{A_{ij} e^{i\phi}\}, \tag{7}$$

where A_{ij} represents the amplitude and ϕ the phase of GWs,

$$\phi = k_\mu x^\mu = g_{\mu\nu} k^\mu x^\nu, \tag{8}$$

with x^μ the point of spacetime which the waves currently pass.

3 THE ANNULAR WAVEGUIDE

Consider an annular waveguide in the shape of a torus, as shown in Figure 2. Its radius is R, and the cross section is a rectangle with sides $a > b$, both being much less than R, say, $a, b \sim 1$ cm, and $R \sim 1$ m. Note that the waveguide actually used by Cruise & Ingley (2005, 2006) actually has the shape of a rectangle, instead of a torus. For simplicity of analysis, here we consider a torus since the working mechanism is the same. Inside the torus one can input a beam of linearly polarized EW propagating around the toroidal loop, which consists of a TE_{10} mode (transverse electric field) with the electric field $\boldsymbol{E}$ pointing along the x^3-axis. The EWs are microwaves, e.g., with a wavelength $\lambda_e \sim 1$ mm and a frequency $\nu_e = c/\lambda_e \sim$

10^{11} Hz. The guided EWs of the TE_{10} mode in the torus travel around the loop at a group speed (Li et al. 1997),

$$v = c\sqrt{1 - (\frac{\lambda_e}{2a})^2}, \tag{9}$$

where c is the speed of light, and v is very close to c. For instance, for $\lambda_e \sim 1\,\mathrm{mm}$ and $a = 1\,\mathrm{cm}$, the difference between the two is $\sim (\lambda_e/2a)^2/2 \sim 10^{-3}$. As is well-known, for a TE_{10} mode to exist in the waveguide, one has to have $\lambda_e \le 2a$. The angular velocity of the EWs cycling around the loop is then

$$\omega_0 = \frac{v}{R} \simeq \frac{c}{R}\,. \tag{10}$$

As will be seen below, when the angular frequency ω of the incident GWs is very close to ω_0, i.e., when at the resonant condition, the detector responds most sensitively to the GWs. Therefore, such a device of given radius R will primarily detect GWs of a resonant frequency around

$$\nu_g \simeq \frac{c}{2\pi R}\,. \tag{11}$$

For example, if the radius is $R = 1\,\mathrm{m}$, the frequency of GWs to be detected is $\nu_g \simeq 5 \times 10^7$ Hz, three or four orders smaller than ν_e. The frequency of GWs to be detected can be varied by adjusting the size R, which is an advantage. For the 4-d spacetime, one can choose a coordinate system $\{x^\mu\}$ with $\mu = 0, 1, 2, 3$ and $x^0 \equiv ct$, such that the waveguide lies on the (x^1, x^2) plane, see Figure 2. Note that the geometric size R of the waveguide is negligibly small in comparison with the Hubble radius, $\sim c/H$, so the effect of cosmic expansion on the torus can be totally neglected.

We consider a beam of GWs passing through the detector. Assume the wavelength λ_g of GWs is much longer than that of of the EWs in the waveguide, λ_e, i.e., $\lambda_g \gg \lambda_e$, so that the geometric optics approximation applies in describing the EWs (Cruise 1983; Misner et al. 1973). In fact, this assumption on the incident GWs is automatically satisfied if the GWs satisfy the resonant condition. The PV of the linearly polarized EWs can be described by a 4-vector, $\Pi^\mu = (\Pi^0, \Pi^1, \Pi^2, \Pi^3)$, which is real and normal to the wave vector P^μ of the EWs

$$\Pi_\mu P^\mu = 0\,, \tag{12}$$

and satisfies the normalized condition (Misner et al. 1973; Cruise 1983)

$$\Pi_\mu \Pi^\mu = 1\,. \tag{13}$$

Equation (12) shows that one can add a multiple of P^μ to Π^μ without affecting any physical measurements (Misner et al. 1973), since P^μ is a null vector with $P_\mu P^\mu = 0$. Suppose that the EWs are propagating along the x^1-axis with wave vector $P^\mu = (P^0, P^1, 0, 0)$, which satisfies $P_\mu P^\mu = 0$. Then by Equation (12), the PV of the EWs can be generally written as $\Pi^\mu = (\kappa P^0, \kappa P^1, \Pi^2, \Pi^3)$, where κ is an arbitrary constant. Then, Equation (13) leads to

$$|\Pi^2|^2 + |\Pi^3|^2 = 1. \tag{14}$$

Since initially the electric field $\boldsymbol{E}$ of EWs inside the torus is set to be along the x^3- axis and Π^i is, by definition, in the direction of $\boldsymbol{E}$, so the initial PV is

$$\Pi^\mu = (\,0, 0, 0, 1), \tag{15}$$

i.e., initially the PV has a vanishing $\Pi^2 = 0$ component.

However, the presence of GWs will cause a rotation of the Π^μ about the direction of propagation, generating a non-vanishing $\Pi^2 \neq 0$ i.e., a component $E^2 \neq 0$ of the electric field $\boldsymbol{E}$ of the EWs in the waveguide. One puts an electric field probe inside the waveguide at the intersection of the x^2- axis and the torus. The probe is on the line of x^2-axis, so it can probe the non-vanishing electric field $\boldsymbol{E}^2$ due to the rotation of $\boldsymbol{E}$ caused by the GWs (Cruise & Ingley 2005, 2006). The GWs induce an electric voltage on the electric probe $V = E_0 \alpha\, l\, \sin{(2\pi\nu_e t)}$, where E_0 is the TE_{10} mode electric field in the waveguide, l is the length of the conducting probe.

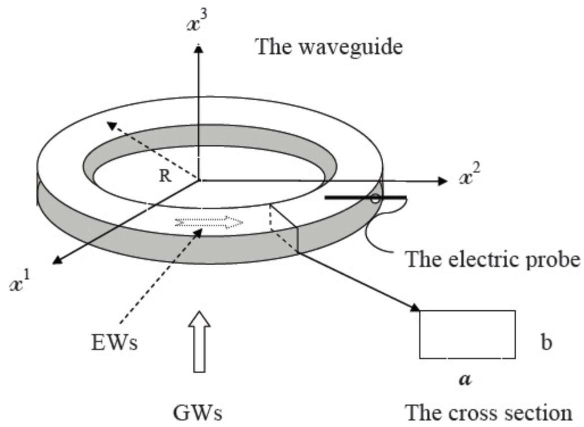

Fig. 2 A sketch of the annular waveguide. The cross section of the waveguide is a rectangle with side a and b which are much smaller than the radius R. EWs travel inside the waveguide and GWs propagate along the x^3-axis.

In the geometric optics approximation, the motion of Π^μ is described as being parallel-propagating along the rays of EWs with the equation

$$\frac{d\Pi^\mu}{ds} + \Gamma^\mu_{\nu\sigma}\Pi^\nu \frac{dx^\sigma}{ds} = 0, \tag{16}$$

where s is an affine parameter, which can be chosen to be $s = t/T_0$ with $T_0 = 2\pi/\omega_0$ the period of the EWs traveling around the torus. Note that when s goes from 0 to 1, EWs go one cycle around the torus. Since $a, b \ll R$, one can view the EWs in the waveguide as travelling along the $1-$dimensional loop path,

$$x^\mu = R\left(\frac{2\pi cs}{v}, -\sin 2\pi s, \cos 2\pi s, 0\right), \tag{17}$$

where v is the group speed of EWs.

With the initial setup of the polarization of EWs in the torus, we only need to consider the component Π^2 of the polarization.

4 CHANGE OF Π^2

Even the setup of the waveguide detector is fixed in the laboratory, GWs in space can come in any direction at random. Therefore, we need to determine the rotation of polarization of EWs caused by GWs travelling along the directions x^i, $i = 1, 2, 3$, respectively.

4.1 GWs Travelling along the Positive x^3-axis

Consider a beam of monochromatic plane GWs travelling along the positive x^3-axis with wave vector $k^\mu = (2\pi/\lambda_g, 0, 0, 2\pi/\lambda_g)$. As the GWs pass the annular waveguide whose position is given by Equation (17), substituting it into Equation (8) will yield the phase of the GWs at the point inside the annular waveguide,

$$\phi = -2\pi s\,\omega/\omega_0. \tag{18}$$

Here $\omega = 2\pi c/\lambda_g$ represents the angular frequency of the GWs, and $\omega_0 = (2\pi/T_0)$ is the cycling angular frequency of the EWs around the torus. One can take the flat spacetime slightly perturbed by the GWs to represent the local region of the waveguide. In the transverse traceless (TT) gauge, the metric tensor can be written as

$$g_{\mu\nu} = \eta_{\mu\nu} + h_{\mu\nu} = \begin{pmatrix} -1 & 0 & 0 & 0 \\ 0 & 1+h_\oplus & h_\otimes & 0 \\ 0 & h_\otimes & 1-h_\oplus & 0 \\ 0 & 0 & 0 & 1 \end{pmatrix},$$

and

$$g^{\mu\nu} = \eta^{\mu\nu} - h^{\mu\nu} = \begin{pmatrix} -1 & 0 & 0 & 0 \\ 0 & 1 - h_\oplus & -h_\otimes & 0 \\ 0 & -h_\otimes & 1 + h_\oplus & 0 \\ 0 & 0 & 0 & 1 \end{pmatrix},$$

where $h_\oplus$ and $h_\otimes$ denote the $+$ and $\times$ modes of polarization of the GWs, respectively. In general, these two modes may not be coherent, i.e. their phases are random and independent, similar to the natural light of EWs. If they have the same phase ϕ, which is known as the *linearly* polarized GWs (Misner et al. 1973), then by Equation (7) one has

$$h_\oplus = A_\oplus \cos\phi, \quad h_\otimes = A_\otimes \cos\phi, \tag{19}$$

where $A_\oplus$ and $A_\otimes$ are real numbers.

As can be checked, the change in Π^3 due to the GWs is of order of $|h_{ij}|^2$, so in the subsequent calculation $\Pi^3 = 1$ is assumed. To calculate the change of Π^2 up to the linear order of h_{ij}, one needs the following Christoffel components,

$$\begin{aligned} \Gamma^2_{31} &= -\pi A_\otimes \sin\phi/\lambda_g, \\ \Gamma^2_{32} &= \pi A_\oplus \sin\phi/\lambda_g, \end{aligned} \tag{20}$$

the other components are either zero or of order $|h_{ij}|^2$, having no contributions. Integrating Equation (16) gives an expression of the change in Π^2 around one circle of the torus,

$$\Delta\Pi^2 = \int_0^1 \frac{d\Pi^2}{ds} ds = -\int_0^1 \left(\Gamma^2_{31}\Pi^3 \frac{dx^1}{ds} + \Gamma^2_{32}\Pi^3 \frac{dx^2}{ds} \right) ds. \tag{21}$$

Substituting Equations (17) and (20) into the integration, one has

$$\Delta\Pi^2 = \frac{2\pi^2 R}{\lambda_g} \int_0^1 \left(A_\otimes \sin\left(2\pi s \frac{\omega}{\omega_0}\right) \cos 2\pi s - A_\oplus \sin\left(2\pi s \frac{\omega}{\omega_0}\right) \sin 2\pi s \right) ds. \tag{22}$$

Carrying out the integration results in

$$\Delta\Pi^2 = \frac{A_\otimes}{2} \left(1 - \cos(2\pi\varpi)\right) \frac{\varpi^2}{\varpi^2 - 1} - \frac{A_\oplus}{2} \sin(2\pi\varpi) \frac{\varpi}{\varpi^2 - 1}, \tag{23}$$

where $\varpi \equiv \omega/\omega_0$. So the change of Π^2 depends on ω.

Let us see what value $\Delta\Pi^2$ will take when the cycling angular frequency of the EWs is equal to the angular frequency of the GWs, i.e., at the resonant condition,

$$\omega_0 = \omega. \tag{24}$$

Taking the limit $\varpi \to 1$ in Equation (23) yields a constant value

$$\Delta\Pi^2 = -\frac{\pi A_\oplus}{2}, \tag{25}$$

which has only contribution from the $+$ mode. This is a known result in Cruise (2000).

We now check other special cases of Equation (23).

(1) If GWs are given such that $A_\oplus = 0$, i.e., there is only the $\times$ mode, then

$$\Delta\Pi^2 = \frac{A_\otimes}{2} \left(1 - \cos(2\pi\varpi)\right) \frac{\varpi^2}{\varpi^2 - 1}, \tag{26}$$

See Figure 3. It is shown that $\Delta\Pi^2$, as a function of ϖ, can be both positive and negative. A maximum value of $\Delta\Pi^2$ is reached at $\varpi \simeq 1.434$.

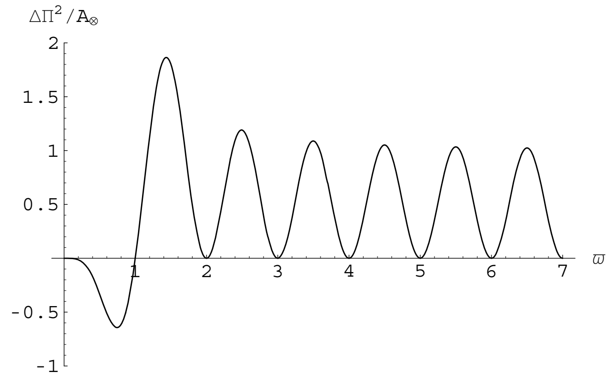

Fig. 3 $\Delta\Pi^2$ as an oscillating function of ϖ when $A_\oplus = 0$, showing a maximal value of $1.864A_\otimes$ at $\varpi = 1.434$ and a minimal value of $-0.643A_\otimes$ at $\varpi = 0.743$. Note that (1) $\Delta\Pi^2 = A_\otimes$, for $\varpi \gg 1$ and ϖ half integers; (2) $\Delta\Pi^2 = 0$, for ϖ integers; (3) $\Delta\Pi^2 = 0$, for $\varpi \to 0$.

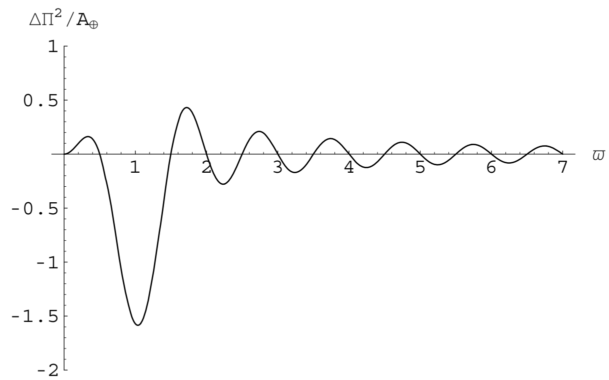

Fig. 4 $\Delta\Pi^2$ as a function of ϖ when $A_\otimes = 0$, which has a minimum $-1.585A_\oplus$ at $\varpi = 1.036$.

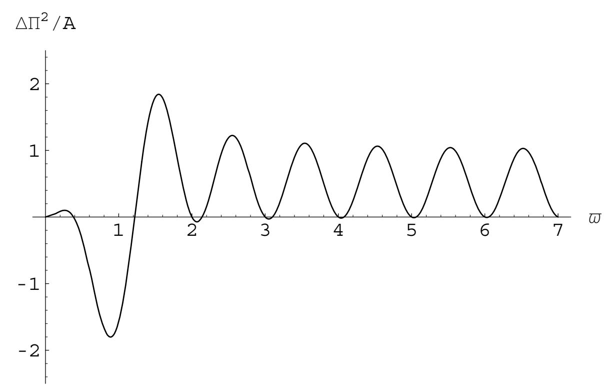

Fig. 5 $\Delta\Pi^2$ as a function of ϖ when $A_\otimes = A_\oplus = A$, showing a maximum 1.842 at $\varpi = 1.546$ and a minimum -1.802 at $\varpi = 0.889$.

(2) If there is only the + mode,

$$\Delta\Pi^2 = -\frac{A_\oplus}{2}\sin(2\pi\varpi)\frac{\varpi}{\varpi^2 - 1}, \tag{27}$$

then we have the result shown in Figure 4. A minimum value of $\Delta\Pi^2$ is reached at $\varpi \simeq 1.036$.

(3) If $A_\otimes = A_\oplus = A$, where A is real, as is likely the case for relic gravitational waves, then one obtains

$$\Delta\Pi^2 = \frac{A}{2}(\varpi - \varpi\cos(2\pi\varpi) - \sin(2\pi\varpi))\frac{\varpi}{\varpi^2 - 1}. \tag{28}$$

See Figure 5, which is compounded of Figures 3 and 4.

Instead of a linearly polarized GWs in Equation (19), we consider the case of circularly polarized GWs with $A_\oplus = iA_\otimes = A$,

$$h_\oplus = A\cos\phi, \quad h_\otimes = A\sin\phi\,. \tag{29}$$

By similar calculations, one has the relevant Christoffel components,

$$\Gamma^2_{31} = \pi A\cos\phi/\lambda_g\,,$$
$$\Gamma^2_{32} = \pi A\sin\phi/\lambda_g\,. \tag{30}$$

Integrating Equation (21) yields

$$\Delta\Pi^2 = \frac{A\varpi\sin(2\pi\varpi)}{2(1+\varpi)}, \tag{31}$$

which is shown in Figure 6.

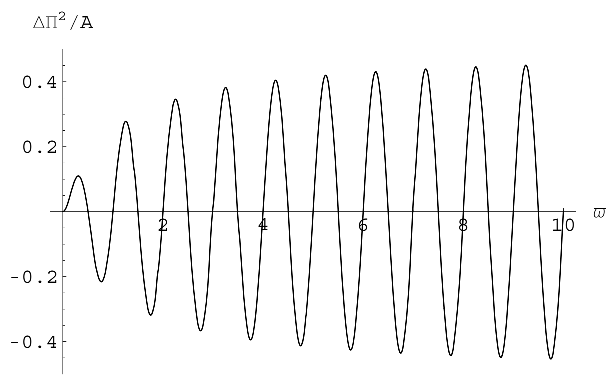

Fig. 6 Relation between $\Delta\Pi^2$ and ϖ for circularly polarized GWs. The value of $\Delta\Pi^2$ will always be less than $A/2$.

4.2 GWs Travelling along the Positive x^1-axis

Different from the above, now consider a plane GW travelling along the positive x^1-axis. The wave vector is $k^\mu = 2\pi/\lambda_g(1, 1, 0, 0)$. By Equations (8) and (7) the phase of the GW in the torus is

$$\phi = -2\pi x^0/\lambda_g + 2\pi x^1/\lambda_g = -(2\pi s + \sin(2\pi s))\omega/\omega_0. \tag{32}$$

The metric is now

$$g_{\mu\nu} = \eta_{\mu\nu} + h_{\mu\nu} = \begin{pmatrix} -1 & 0 & 0 & 0 \\ 0 & 1 & 0 & 0 \\ 0 & 0 & 1 + h_\oplus & h_\otimes \\ 0 & 0 & h_\otimes & 1 - h_\oplus \end{pmatrix}.$$

Similar calculations give the relevant Christoffel components

$$\begin{aligned}\Gamma^2_{30} &= \pi A_\otimes \sin\phi/\lambda_g,\\ \Gamma^2_{31} &= -\pi A_\otimes \sin\phi/\lambda_g,\end{aligned} \tag{33}$$

and the change in Π^2 around one circuit of the path

$$\Delta\Pi^2 = \frac{2\pi^2 r A_\otimes}{\lambda_g}\int_0^1 (1+\cos(2\pi s))\sin\left(\frac{\omega}{\omega_0}(2\pi s+\sin(2\pi s))\right)ds. \tag{34}$$

Integrating Equation (34) gives rise to

$$\Delta\Pi^2 = A_\otimes \sin^2(\pi\varpi). \tag{35}$$

This oscillates between $A_\otimes$ and 0. Note that $A_\oplus$ makes no contribution.

In the case of circularly polarized GWs, Equations (33) and (34) should be replaced by

$$\begin{aligned}\Gamma^2_{30} &= -\pi A\cos\phi/\lambda_g,\\ \Gamma^2_{31} &= \pi A\cos\phi/\lambda_g,\end{aligned} \tag{36}$$

and

$$\Delta\Pi^2 = \frac{2\pi^2 r A}{\lambda_g}\int_0^1 (1+\cos(2\pi s))\cos\left(\frac{\omega}{\omega_0}(2\pi s+\sin(2\pi s))\right)ds, \tag{37}$$

and one has

$$\Delta\Pi^2 = \frac{A}{2}\sin(2\pi\varpi), \tag{38}$$

oscillating between $A/2$ and $-A/2$.

4.3 GWs Travelling along the Positive x^2-axis

When plane GWs travel along the positive x^2-axis, the metric tensor of spacetime is

$$g_{\mu\nu} = \eta_{\mu\nu} + h_{\mu\nu} = \begin{pmatrix} -1 & 0 & 0 & 0\\ 0 & 1+h_\oplus & 0 & h_\otimes\\ 0 & 0 & 1 & 0\\ 0 & h_\otimes & 0 & 1-h_\oplus \end{pmatrix}.$$

Similar calculations show that the relevant Christoffel components are 0, and thus

$$\Delta\Pi^2 = 0. \tag{39}$$

Thus, GWs travelling along the x^2-axis will not change Π^2. Therefore, to avoid a null result of detection in case of an incident GWs in the x^2 direction, one should put two probes with 90^0 separation along the annular waveguide.

5 CUMULATIVE EFFECT

When EWs pass n cycles along the annular waveguide, the change of Π^2 may be accumulative. This is of practical significance in actual detections. We need only consider GWs along the x^3- and x^1- directions.

First, for the linearly polarized incident GWs in the x^3- direction, integrating Equation (22) form 0 to n gives the change of Π^2 for n cycles

$$(\Delta\Pi^2)_n = \frac{A_\otimes}{2}(1-\cos(2\pi n\varpi))\frac{\varpi^2}{\varpi^2-1} - \frac{A_\oplus}{2}\sin(2\pi n\varpi)\frac{\varpi}{\varpi^2-1}. \tag{40}$$

For the special case $A_\otimes = 0$, Figure 7 gives a plot of $(\Delta\Pi^2)_n$ for $n = 10$. In contrast to Figure 6 for $n = 1$, $(\Delta\Pi^2)_n$ is now sharply peaked at $\varpi \simeq 1$ with a much larger amplitude, as a prominent feature. As given in Table 1, under the resonance condition $\varpi \to 1$, the amplitude of $(\Delta\Pi^2)_n$ increases linearly with n. In

Table 1 Case of $A_\otimes = 0$. The amplitude of $(\Delta\Pi^2)_n$ increases linearly with n, as $\varpi \to 1$.

n	$\varpi_{\min}$	$\Delta\Pi^2_{\min}/A_\oplus$
1	1.036	-1.585
10	1.00038	-15.71
100	~ 1	-157.08
1000	~ 1	-1570.8
2000	~ 1	-3141.6
10000	~ 1	-15708

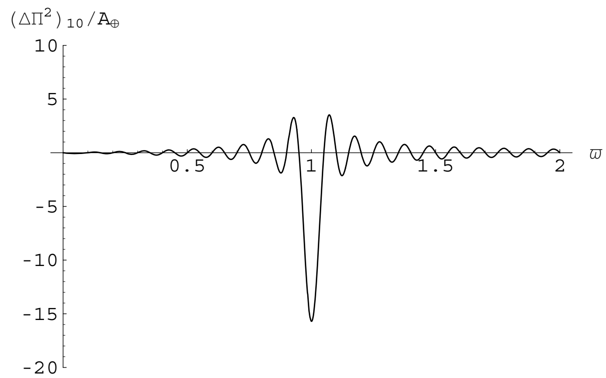

Fig. 7 Case of $A_\otimes = 0$ and $n = 10$. $(\Delta\Pi^2)_n$ has a minimum $-15.071A_\oplus$ at $\varpi = 1.00038$.

Table 2 Case of $A_\oplus = 0$. The amplitudes of extrema of $(\Delta\Pi^2)_n$ increase with n.

n	$\varpi_{\max}$	$\Delta\Pi^2_{\max}/A_\otimes$	$\varpi_{\min}$	$\Delta\Pi^2_{\min}/A_\otimes$
1	1.434	1.864	0.743	–0.643
10	1.038	12.027	0.964	–10.761
100	1.0037	114.456	0.9963	–113.189
1000	1.00037	1138.85	0.99963	–1137.58
2000	1.00019	2277.07	0.99982	–2275.8
10000	1.00004	11382.8	0.999963	–11381.5

fact, this linearly-increasing amplitude $\Delta\Pi^2_{\min}$ at very large n is also obtained by taking the resonance limit $\varpi \to 1$ in Equation (40), which yields

$$(\Delta\Pi^2)_n = -\frac{n\pi A_\oplus}{2}, \tag{41}$$

which is in accord with the result obtained by Cruise (2000).

The special cases of $A_\oplus = 0$ and of $A_\oplus = A_\otimes$ are quite similar to each other. $(\Delta\Pi^2)_n$ has, for each given n, both a sharp maximum $\Delta\Pi^2_{\max}$ at $\varpi_{\max} > 1$ and a sharp minimum $\Delta\Pi^2_{\min}$ at $\varpi_{\min} < 1$. As $n \to \infty$, the amplitudes $\Delta\Pi^2_{\max}$ and $\Delta\Pi^2_{\min}$ increase with n approximately linearly, and their locations $\varpi_{\max}$ and $\varpi_{\min}$ approach 1 from either side, respectively. Figures 8 and 9 show $(\Delta\Pi^2)_n$ with $n = 10$ for $A_\oplus = 0$ and for $A_\oplus = A_\otimes$, respectively. Tables 2 and 3 list the increase with n of the amplitudes of extrema $\Delta\Pi^2_{\max}$ and $\Delta\Pi^2_{\min}$ for $A_\oplus = 0$ and for $A_\oplus = A_\otimes$, respectively.

For circularly polarized GWs in the x^3- direction, the n- cycle result is

$$(\Delta\Pi^2)_n = \frac{A\varpi\sin(2\pi n\varpi)}{2(1+\varpi)}, \tag{42}$$

which does not accumulate with n, but vibrates more rapidly than Equation (31).

Table 3 Case of $A_\oplus = A_\otimes$. The amplitudes of extrema of $(\Delta\Pi^2)_n$ increase with n.

n	$\varpi_{\max}$	$\Delta\Pi^2_{\max}/A_\otimes$	$\varpi_{\min}$	$\Delta\Pi^2_{\min}/A_\otimes$
1	1.546	1.842	0.889	–1.802
10	1.055	11.05	0.982	–20.214
100	1.0055	103.504	0.9981	–205.148
1000	1.00055	1028.1	0.99981	–2054.59
2000	1.00027	2055.43	0.999907	–4109.52
10000	1.00005	10274.1	0.999981	–20549

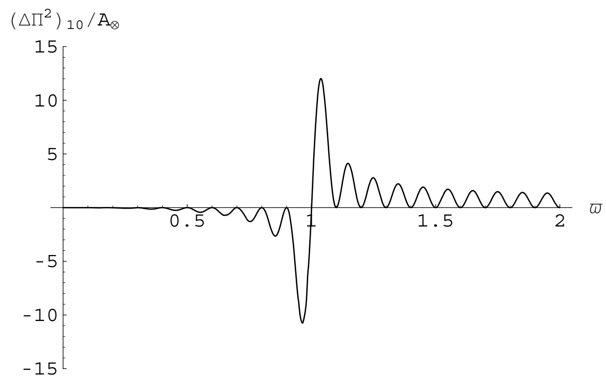

Fig. 8 Case of $A_\oplus = 0$ and $n = 10$. $\Delta\Pi^2_{\max} = 12.027 A_\otimes$ at $\varpi = 1.038$, and $\Delta\Pi^2_{\min} = -10.761 A_\otimes$ at $\varpi = 0.964$.

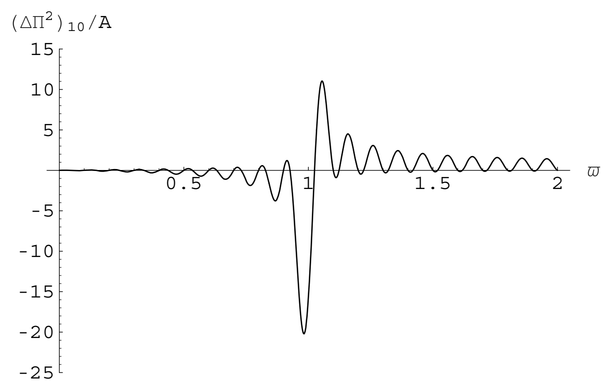

Fig. 9 Case of $A_\otimes = A_\oplus = A$ and $n = 10$. $\Delta\Pi^2_{\max} = 11.05A$ at $\varpi = 1.055$, and $\Delta\Pi^2_{\min} = -20.214A$ at $\varpi = 0.982$.

Secondly, for the lineal polarized incident GWs in the x^1- direction, the n- cycle result is

$$(\Delta\Pi^2)_n = A_\otimes \sin^2 (n\pi\varpi), \tag{43}$$

which shows no accumulating effect. For the circularly polarized GWs in the x^1- direction,

$$(\Delta\Pi^2)_n = \frac{A\sin(2n\pi\varpi)}{2}, \tag{44}$$

without any accumulating effect either.

So the above detailed analysis on the n-cycle accumulating effect yields a simple conclusion: Only linearly polarized incident GWs in the x^3-axis has a linearly accumulating effect on the rotation of the PV of the EWs in the limit $\varpi \to 1$. In order to experimentally obtain a maximum effect of n-cycle accumulation, the circling EWs in the waveguide should be running so that n is as large as possible. Of course, due to attenuation of EWs in actual waveguides, for a given waveguide made of conducting metal, such as copper, an input beam of EWs in the waveguide can run only a finite number of turns around the torus. The maximum value of n is approximately equal to the quality factor Q, mainly determined by the conducting metal employed and the pump resonances. For instance, Cruise's group (Cruise & Ingley 2005, 2006) has used copper for the waveguide, and the measured value of the quality factor $Q \simeq 2000$. As for the selective response of the detector to the particular x^3- direction of the incident GWs under the resonant condition $\omega \simeq \omega_0$, it is a problem for gravitational radiations from certain sources, since they generally exist for a finite short period of time (from minutes to hours) and have some fixed direction of propagation. However, for the RGWs as the detection object, it is not a problem at all, as they consist of various modes in all directions and of all frequencies, and they are a stochastic background existing everywhere and at all time. Therefore, RGWs serve as a natural object of detection. What one needs to do is to set up a convenient position of the torus and to fix the the cycling angular frequency $\omega_0 = v/R$ of EWs around the waveguide. There are always modes of RGWs in the x^3- direction with angular frequency $\omega \simeq \omega_0$.

6 CAPABILITY FOR DETECTING VERY HIGH FREQUENCY RGWS

We examine the capability of the waveguide detector built up by Cruise & Ingley (2005, 2006) particularly in regards to RGWs. Consider the favorable case of GWs travelling along the x^3-direction. Since the rotation $\Delta\Pi^2$ is small, it is equal to the rotated angle α, $\alpha \simeq \Delta\Pi^2$. This angle can be measured by the electric probe. In general the detector sensitivity will be limited by thermal noise in the electronic amplifiers. It has been found that the minimum detectable angle of rotation is (Cruise & Ingley 2006)

$$\alpha_{\min} = \sqrt{\frac{ab\,kTB}{fPl^2}}, \tag{45}$$

where f is an efficiency factor of the probe transferring electric signals to the following electronic amplifiers, k the Boltzmann constant, T the amplifier noise temperature, and B the detector bandwidth in Hertz. Thus, for a constant amplitude on the time scale $\sim Q/\nu_0$, during which the EWs travel Q turns around the loop. By Equation (41) the minimum detectable amplitude $h_{\min}$ of the GWs is

$$h_{\min} = \frac{2}{\pi}\frac{\alpha_{\min}}{Q} = \frac{2}{\pi}\sqrt{\frac{abkTB}{fP_{\rm in}Q^3l^2}}, \tag{46}$$

where the input power $P_{\rm in}$ is related to the circulating power P by $P_{\rm in} = P/Q$, Q being the quality factor of the waveguide. For a random signals of GWs with amplitude varying considerably over the time scale $\sim Q/\nu_0$, the minimum detectable amplitude is

$$h_{\min} = \frac{2}{\pi}\sqrt{\frac{abkTB}{fP_{\rm in}Q^2l^2}}, \tag{47}$$

since the angle α of rotation accumulatively increases as $\alpha \propto \sqrt{Q}$, as for a random walk.

The waveguide detector is used to monitor GWs of frequency $\sim 10^8$ Hz, which primarily come from the stochastic background of RGWs with a very broad frequency range $(10^{-18} \sim 10^{10})$ Hz (Grishchuk 2001; Zhang et al. 2005a,b, 2006). The RGW spectrum $h(\nu, \eta_H)$ as given by Equation (6) in a frequency range $> 10^7$ Hz depends sensitively on the reheating parameter β_s. The spectra for three different values of $\beta_s = 0.5, 0, -0.3$, respectively, are given in Figure 10 for a model with $\beta = -1.8$, $r = 0.22$, and $\Omega_A = 0.75$. A larger β_s has a lower amplitude in the range $10^7 \sim 10^9$ Hz, but around $\nu \geq 10^9$ Hz the spectrum begins to increase considerably. Therefore, if the detector can accurately detect the RGWs signals, it will, in principle, be able to constrain the model parameters β and β_s, and distinguish different models of reheating during the early universe.

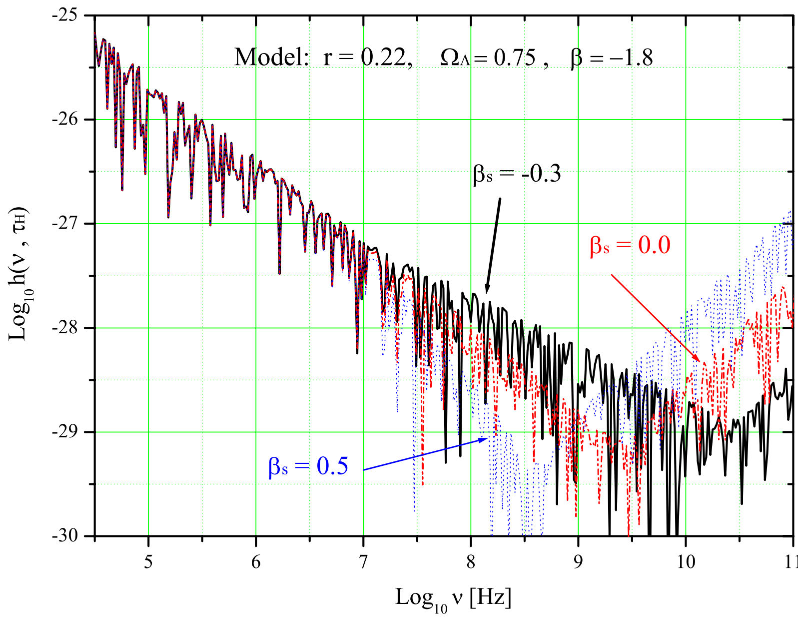

Fig. 10 Spectrum of $h(\nu, \eta_H)$ with different parameter β_s for $\beta = -1.8$.

Other sources of GWs, such as binary neutron stars or black holes, merging of neutron stars or black holes, can produce GWs, but the frequency is much lower than 10^8 Hz (Zhang et al. 2004). Thus they cannot be detected by the waveguide detector discussed here. There might be other astrophysical processes, which can give rise to high frequency GWs. Thermal gravitational radiation of stars can generate GWs at most probable frequencies $\sim 10^{15}$ Hz (Bisnovatyi & Rudenko 2004; Weinberg 1972), but this frequency is too high for the waveguide detector. The predicted grazer beams in interstellar plasma can generate GWs with "optical" frequencies $> 10^{12}$ Hz, which are still too high for the waveguide detector (Servin & Brodin 2003). The GW radiation from primordial black holes of $M \leq 10^{-5} M_\odot$ can generate GWs with frequencies $\geq 10^{10}$ Hz, which are also too high for the waveguide detector, and the rate of event is very low ($\sim 5 \times 10^{-2}$ year^{-1} galaxy^{-1}, Nakamura et al. 1997). Therefore, our primary object of detection is RGWs, whose spectrum in the current accelerating universe has been derived, e.g., Zhang et al. (2005a,b, 2006) and Miao & Zhang (2007).

What the waveguide detector actually detects is the root-mean-square (r.m.s.) amplitude of RGWs per Hz$^{1/2}$ at a given ν, which can be written simply as (Grishchuk 2001)

$$\frac{h(\nu)}{\sqrt{\nu}}, \tag{48}$$

where $h(\nu)$ denotes the value of the spectrum $h(\nu, \eta_H)$ given in Equation (6). Since the waveguide detector works around frequency 10^8 Hz, so we need to examine $h(\nu, \eta_H)$ around this frequency predicted by the calculations (Zhang et al. 2005a,b, 2006; Miao & Zhang 2007). For a cosmological model with the tensor/scalar ratio $r = 0.22$, dark energy $\Omega_\Lambda = 0.75$, and reheating parameter $\beta_s = 0.3$, one can read from Figure 1 the values $h(\nu) \simeq 10^{-28}, 10^{-34}$ for inflationary parameter $\beta = -1.8, -2.02$, respectively. Then the corresponding r.m.s amplitude per Hz$^{1/2}$ at $\nu = 10^8$ Hz is

$$\frac{h(\nu)}{\sqrt{\nu}} \simeq (10^{-32},\ 10^{-37})\ \mathrm{Hz}^{-1/2}, \tag{49}$$

for the two values of β, respectively. On the other hand, the detector sensitivity can be improved by using the cross correlation of two or more detectors. From a short run of 4 seconds of two detectors, Cruise &

Ingley (2006) gave the cross correlation sensitivity,

$$5 \times 10^{-15} \text{Hz}^{-1/2}, \tag{50}$$

which is within a factor 4 of the predicted sensitivity for parameters $P_{\rm in} = 69\,\text{mW}$, $T = 300\,\text{K}$, $Q = 2000$, $(ad)/l^2 = 0.5$, and $f > 0.9$. Comparing the preliminary experimental result in Equation (50) with the predicted values, it is shown that the predicted value of RGWs in the model $\beta = -1.8$ is lower than the prototype detector sensitivity by 17 orders. As has been analyzed in Cruise & Ingley (2006), the detector sensitivity of the current detector could be improved by a factor of $10^4 \sim 10^5$, by taking advantage of optimization of the transducers, cryogenic amplifiers and multiple detector correlation, but even with these improvements, there still are 12 orders short to measure the predicted amplitude of RGWs in Equation (49).

An interesting feature of the spectrum of RGWs is that it has a higher amplitude in lower frequencies. This may be suggestive for new ways of enhancing the chance of detections. As is seen from Equation (11), if one increases the radius R of the annular waveguide, e.g., from 1 meter to 100 meters, the frequency of GWs to be detected will subsequently be reduced to a low value $\nu_g \simeq 5 \times 10^5\,\text{Hz}$, at which the spectral amplitude $h(\nu, \eta_H)$ increases by a factor $\sim 10^3$, as is seen from Figure 1, and the r.m.s amplitude per $\text{Hz}^{1/2}$ will be $h(\nu)/\sqrt{\nu} \sim 10^{-28}\,\text{Hz}^{-1/2}$. Now, it is only 8 orders lower than the detector sensitivity of the improved device. Therefore, according to our calculation of the RGWs, it is unlikely to detect signals of RGWs using the annular waveguide detectors as they stand today, but enlarging the radius R will enhance the detection probability considerably, of course this involves a larger cost and a more complex construction. Note that LIGO is still unable to detect the RGWs by 2 orders of magnitude, even though it has achieved its design sensitivity (Miao & Zhang 2007). Moreover, there are possibilities that the waveguide detector can detect signals from other kinds of sources of GWS with a much improved sensitivity.

7 CONCLUSIONS

From the calculations of the rotation of the PV of EWs, it is found that, essentially, the detector only responds to linearly polarized RGWs travelling in the x^3-axis under the resonant condition. Both circularly polarized RGWs travelling along any direction and linearly polarized RGWs travelling along the x^1- or x^2-axis give no observable clues, but these will not cause any problem when the object of detection is RGWs.

From our analysis comparing the RGWs spectrum with the detector sensitivity, we find that the RGWs in the accelerating universe have a very low amplitude and are not possible to detect using the current detector. The gap between them is some 17 orders of magnitude under the current experimental conditions. Even with the improvements on the current detector system as planned in 2005, there will still be a gap of 12 orders of magnitude. Focusing on the detector itself, Equations (46) and (47) show that the sensitivity of the detector can be directly improved by several means: (1) by using cryogenic devices at temperature T lower than that of the environment, i.e., to reduce thermal noise of the amplifiers; (2) by increasing the quality factor Q of the waveguide, so the EWs can travel more number of turns around the loop, (3) by increasing the input power $P_{\rm in}$ of the EWs into the waveguide; (4) by using multiple detectors, whose correlation can improve the sensitivity of the detector. On the other hand, the shape of the RGW spectrum $h(\nu)$ is such that its amplitude is higher in lower frequencies. Therefore, it may be more promising to detect RGWs in a relatively lower frequency range. For instance, if the radius of the torus is increased to $R = 100$ meter, the detecting frequency $\nu_g \sim 5 \times 10^5\,\text{Hz}$, and the gap will reduced down to 8 orders of magnitude. An overall estimate is that significant improvements of the current prototype detector are needed for a possible detection of RGWs.

Acknowledgements We thank Dr. A.M. Cruise for helpful suggestions. Y. Zhang's work was supported by the NSFC (Grant 10773009), SRFDP and CAS.

References

Abramovici A. et al., 1992, Science 256, 325
Allen Z. et al., 2000, Phys. Rev. Lett, 85, 5046
Aston P. et al., 2001, Class. Quant. Grav, 18, 243
Baskaran D., Grishchuk L. P., Polnarev A. G., 2006, Phys. Rev. D, 74, 083008
Bisnovatyi-Kogan G. S., Rudenko V. N., 2004, Class. Quantum. Grav., 21, 3347
Bradaschia C. et al., 1990, Nucl. Instrum. Methods Phys. Res. A, 289, 518
Cruise A. M., 1983, MNRAS, 204, 485;
Cruise A. M., 2000, Class. Quantum. Grav, 17, 2525
Cruise A. M., Ingley R. M. J., 2005, Class. Quantum. Grav, 22, s479
Cruise A. M., Ingley R. M. J., 2006, Class. Quantum. Grav, 23, 6185 bibitem[1974]GaltsovGaltsov D. V., Gratz Yu., 1974, Sov. Phys.–JETP, 17, 94
Giovamini M., 1999, Class.Quant.Grav., 16, 2905
Giovamini M., 1999, Phys. Rev. D, 60, 123511
Grishchuk L. P., 1975, Sov. Phys. JETP, 40, 409
Grishchuk L. P., 1997, Class. Quantum. Grav., 14, 1445
Grishchuk L. P. et al., 2001, Phys. Usp., 44, 1
Grishchuk L. P., 2001, Lecture Notes in Physics, 562, 167,
Hulse R. A., Taylor J. H., 1975, ApJ, 195, L51
Jafry Y., Corneliss J., Reinhard R., 1994, ESA Bull, 18, 219
Kamionkowski M., Kosowsky A,, Stebbins A., 1997, Phys. Rev. D, 55, 7368
Li C. Z., Zhao F. Z., 1997, Electrodynamics Tutorial, (Publishing Company of National University of Defense Technology)
Li F. Y., Tang M. X., Luo J. et al., 2000, Phys. Rev. D, 62, 044018
Li F. Y. et al., 2003, Phys. Rev. D 67, 104008
Li F. Y. et al., 2006, preprint(gr-gc/0604109)
Miao H. X., Zhang Y., 2007, Phys. Rev. D, 75, 104009
Misner C. W., Thorne K. S., Wheeler J. A., 1973, Gravitiation, San Francisco: Freeman, pp.570-580, pp.952-954
Nakamura T. et al., 1997 ApJ, 487, L139
Pritchard L. P., Kaminkowski M., 2005 Ann. Phys.(N.Y.), 318, 2
Seljak U., Zaldarriaga M., 1997; Phys. Rev. Lett, 78, 2054
Servin M., Brodin G., 2003, Phys. Rev. D, 68, 044017
Spergel D. N. et al, 2003, ApJS, 148, 175
Takahashi H., Tagoshi H., the TAMA Collaboration, 2004 Class. Quant. Grav, 21, S697-S702
Weinberg S., 1972, Gravitation and Cosmology, John Wiley & Sons, Inc. New York
Weisberg J. M., Taylor J. H., 2004, In: eds. F. A. Rasio, I. H. Stairs, Binary Radio Pulsars, Proc. Aspen Conference, ASP conf. series,preprint(astro-ph/04071149)
Zhang Y., Zhao W., Yuan Y. F., 2004, Publications of Purple Moutain Observary, 23, 53
Zhang Y., Yuan Y. F., Zhao W. et al, 2005, Class. Quantum. Grav., 22, 1383
Zhang Y. et al., 2005, Chin. Phys. Lett., 22, 1817
Zhang Y., Er X. Z., Xia T. Y. et al., 2006, Class. Quant. Grav., 23, 3783
Zhao W., Zhang Y., 2006, Phys. Rev. D, 74, 043503
Zhao W., Zhang Y., 2006, Phys. Rev. D, 74, 083006